STRUCTURE AND DEVELOPMENT OF VIRUSES AS OBSERVED IN THE ELECTRON MICROSCOPE

VI. ECHO Virus, Type 9*

By RICHARD A. RIFKIND,‡ M.D., GABRIEL C. GODMAN, M.D., CALDERON HOWE, M.D., COUNCILMAN MORGAN, M.D., and HARRY M. ROSE, M.D.

(From the Departments of Microbiology and Medicine, College of Physicians and Surgeons, Columbia University, New York)

Plates 1 to 15

(Received for publication, March 13, 1961)

Cytopathic changes induced in tissue cultures by a variety of enteroviruses have been observed in the light microscope (1–5). Furthermore, detailed analysis by means of electron microscopy has revealed the presence of intracytoplasmic crystalline viral aggregates (6–11) as well as alterations in the fine structure of cells infected by some of these agents (12). A preliminary study of type 9 ECHO virus (1) has demonstrated viral particles in a regular, although non-crystalline, arrangement upon a series of parallel filaments within the cytoplasm of cells manifesting the characteristic enteroviral cytopathic effect. The purpose of this paper is to describe the structure of ECHO 9 virus, the manner in which it develops and the mechanism whereby it gains egress from the infected tissue culture cells.

Methods and Materials

Virus.—Type 9 ECHO (Hill strain) virus was kindly supplied by Dr. Albert B. Sabin.

Cell Cultures.—Rhesus kidney epithelial cells, obtained by trypsinization of normal kidney tissue, were propagated in Melnick's medium (13), a week to 10 days usually sufficing for the development of confluent cell sheets. These were retrypsinized, washed, suspended in fresh medium and dispensed into 25 ml plastic plaque bottles. Fully grown cell sheets were then washed with balanced salt solution, inoculated with 10^3 TCID virus in 0.2 ml of balanced salt solution. After incubation for an hour at 37°C, maintenance medium was added and incubation at 37°C continued. When the desired degree of cytopathic effect was observed the cells were scraped from the bottles into balanced salt solution, centrifuged into pellets, fixed in osmium tetroxide, dehydrated in graded dilutions of ethyl alcohol, embedded in methacrylate, and sectioned as previously described (14). All sections were stained with lead acetate for 30

* These studies were supported by The National Foundation and by the Office of The Surgeon General, Department of the Army, Washington, D.C., under the auspices of the Commission on Influenza, Armed Forces Epidemiological Board.

‡ Fellow of The National Foundation.

minutes according to the method of Dalton and Zeigel (15). Control preparations of uninoculated cells were treated in the same manner. All cultures were screened for hemadsorption agents by the technique of Vogel and Shelokov (16). Preparations represented in this study were devoid of demonstrable simian agents.

RESULTS

Fig. 1 illustrates a cell at a relatively early stage of infection. The nucleus displays a convoluted nuclear membrane and condensed, marginated chromatin. There is a single nucleolus (*Nu*). Adjacent to the nucleus a mass of small, smooth-surfaced, single and multiwalled vesicles displaces the normal cytoplasmic constituents. Some of these vesicles appear empty; others contain material of variable density. Mitochondria (*m*), granule-bearing elements of the endoplasmic reticulum (*er*) and a considerable quantity of free ribonucleoprotein granules are scattered throughout the cytoplasm.

Fig. 2 shows a markedly altered cell which displays a shrunken nucleus (*N*) seemingly the result of loss of nuclear turgor, condensation of the remaining chromatin and collapse of the nuclear membrane. In the cytoplasm two densely packed collections of small granules (*g*), believed, on the basis of histochemical studies (17), to be ribonucleoprotein, lie between the deep folds of the nuclear membrane. A conglomeration of smooth-surfaced vesicles occupies the center of the cell below the nucleus. At the lower left (indicated by arrows) are 4 discrete bodies, each composed of many dense particles in an orderly array. The size, shape, and arrangement of these particles suggests that they are viral and they will be so considered hereafter.

Four viral aggregates similar in appearance to those of Fig. 2 are illustrated at somewhat higher magnification in Fig. 3. The viral particles are aligned in parallel rows traversed by long thin fibrils, 2 to 5 mμ in diameter, which extend freely into the adjacent cytoplasm and merge with a mesh of similar fibrils. One, or more frequently two, fibrils separate the rows of virus. In Fig. 4, which shows the upper aggregate at higher magnification, the viral particles are seen to be of two kinds. Many are extremely dense and in some areas, especially where a slight swelling or displacement has occurred, a delicate outer membrane closely applied to the dense core is apparent (arrows). The average diameter of dense, membrane-coated particles is 22 mμ and the closest center-to-center spacing is approximately 24 mμ. The cores are 13 to 15 mμ in diameter. Other particles consist of roughly circular membranes, about 22 mμ in diameter, containing material of low electron density. These, for reasons to be discussed, will be termed "incomplete virus." Fine filaments course between and beyond the columns of virus.

In the more advanced stage of the cellular lesion seen in Fig. 5, the mitochondria (*m*) are swollen and fragmented and most of the cytoplasmic ground substance is lost. Some distorted, granule-bearing elements of the endoplasmic reticulum (marked *er*) are preserved. Two large viral aggregates are visible, one

near the center and the other in the lower third. Their associated fibrils join a loose network of similar fibrils in the surrounding cytoplasm. Most of the viral particles are of the incomplete variety, but scattered among these are the typical dense forms.

In Fig. 6 the central portion of an infected cell displays a characteristically condensed and convoluted nucleus (*N*), several mitochondria, and smooth-surfaced vesicles. At the lower left is a dense linear body (marked *A*) composed of viral particles which are oriented upon a longitudinal sheaf of fibrils. At the upper left is another viral cluster (marked *B*) which has been sectioned in a plane perpendicular to the course of its fibrils and exhibits a roughly hexagonal outline. This cluster is illustrated at higher magnification in Fig. 7. Although there are scattered defects in the pattern, many of the viral particles are surrounded by 6 adjacent viral particles in a regular hexagonal array. The small punctate densities between the viral particles represent the profiles of cross-sectioned fibrils. Each lies at the center of the equilateral triangle formed by three neighboring viruses. The relationship of virus and fibril is further illustrated in Fig. 8 and its insert. Arrows indicate the typical array of 6 fibrils surrounding one viral particle. In the lower right portion of the cluster many fibrils are indistinct, probably because they are not normal to the plane of section. The third viral array in Fig. 6 (marked *C*) which represents an obliquely transected viral collection, displays neither the longitudinal nor the cross-sectional patterns.

Fig. 9 is believed to illustrate the earliest stages in the formation and ordering of the viral arrays. Six prominent masses of finely granular material are seen in the cytoplasm; four of these (lettered *A* to *D*) are intimately associated with one or more viral aggregates. At the left, two large clusters of virus in characteristic linear arrays originate at the surface of mass *A*. Mass *B* appears to be associated with virus only at one place. Areas *C* and *D* are seen at higher magnification in Fig. 10. On the left a highly ordered, wedge-shaped aggregate of virus is partly buried within the granular mass. Two viral particles display an outer membrane (arrows). Small interparticular densities indicate the presence of the typical fibrillar lattice. Within the mass itself, fine filaments are present. At the right of the picture, viral particles are seen both at the surface and within the finely granular and filamentous matrix.

Two similar sites from another cell are illustrated in Fig. 11. Dense viral particles as well as incomplete forms extend radially in fibril-oriented columns from the surface of both masses. This spatial relationship suggests that the finely granular masses are template sites at which the virus differentiates and becomes aligned upon a fibrillar lattice. The circular inset at the left illustrates one viral particle at sufficient magnification to reveal the peripheral membrane.

Fig. 12 shows part of a cell containing, in the upper half, a rough-surfaced cisternal element of the endoplasmic reticulum whose granules are clearly co-extensive with a large collection of dense particles similar to that shown in Fig. 2 and

believed, on the basis of size, structure, and histochemical correlation (17) to be composed of ribonucleoprotein. The particles, which average 14 mμ in diameter, are irregular in shape, hazy in outline, variable in density, and display no orderly arrangement. In the lower portion of the plate are three transected fascicles of virus. In comparison with the ribonucleoprotein granules, the viral particles are larger, consistently round, uniformly dense, and intimately associated with fibrils. Spatial or structural transition between these two kinds of particles was not encountered. Such observations compel the interpretation that viral particles do not differentiate either from free ribonucleoprotein granules or from the endoplasmic reticulum.

Fig. 13 illustrates a large mass of ribonucleoprotein granules, similar to that shown in Fig. 12. The nucleus (*N*) displays an outer membrane heavily encrusted with granules. An unusually large space, which contains material of moderate density, separates inner and outer nuclear membranes. The nuclear chromatin is highly condensed and appears to be continuous with the cytoplasm in many places. Within the dense chromatin adjacent to the fenestrations in the nuclear membrane localized rarefactions have formed. In some instances the actual sites of communication between nucleus and cytoplasm lie outside the plane of section. Fig. 14 shows a portion of this nucleus, with its fenestrations and their associated rarefactions, at higher magnification.

Fig. 15 shows the peripheral cytoplasm of another cell. A portion of the paranuclear mass of vesicles is seen in the upper right. At the upper border is a group of mitochondria which have many fine dense granules ordered along their cristae. In the lower right several other mitochondria display similar granulation. Two mitochondria from this field are illustrated at higher magnification in Fig. 16. The granules, which measure 8 to 10 mμ, are distinctly smaller than viral or ribonucleoprotein particles or the commonly observed intramitochondrial granules. They are regularly aligned along the surface of the cristae mitochondriales in a manner reminiscent of the arrangement of nucleoprotein particles upon the endoplasmic reticulum. Such mitochondrial granulation has not heretofore been encountered in normal cells nor in cells infected with a variety of other viruses.

In the center of Fig. 15 is a large linear array of viral particles. At the left, indicated by arrows, smaller somewhat more irregular groups of virus appear to be in the process of dispersion. In Fig. 17 the plasma membranes of two adjacent cells traverse the field diagonally. Part of a large aggregate of ribonucleoprotein particles is at the lower left. Two small clusters of virus lie just beneath the bilamellar plasma membrane of the cell on the right (arrows). A group of six viral particles, in the upper third, associated with some amorphous cytoplasmic material, lies in the extracellular space next to a discrete rent in the otherwise continuous plasma membrane of this cell. In the lower third of the picture, three viral particles and a larger mass of cytoplasmic ground substance appear extracellularly adjacent to an extensive zone of discontinuity in the surface mem-

brane of the cell on the left. A larger aggregate of extracellular virus lies close to a disrupted fragment of an apparently avulsed cytoplasmic protrusion in the center of the plate. The delicate outer membranes of several of these particles are shown with particular clarity.

Fig. 18 illustrates the margin of a cell exhibiting numerous small protrusions and two larger cytoplasmic extensions. The lower extension interdigitates with a similar process which must arise from another cell not visible in this section. The nature of the dense material in these processes is not known. A large collection of ribonucleoprotein particles, intimately associated with two flat cisternae of the endoplasmic reticulum, lies at the lower left. On the cell surface there are small clusters of virus (arrows) similar to those in Fig. 17. At the torn base of the large upper cytoplasmic process (labelled *P*) are numerous viral particles lying free in the extracellular space. This area is more clearly seen in Fig. 19. Several particles are still within the cytoplasm but most are free of the cell. The base of the avulsed protrusion is still connected to the cell body by a stalk of naked cytoplasm.

In Fig. 20 the cell has ruptured and a large collection of amorphous cytoplasmic substance, fragmented mitochondria, vacuoles, and numerous small clusters of virus appear to be in the process of release.

DISCUSSION

I. Viral Structure.—

The size of several types of ECHO virus, estimated by a variety of biophysical techniques, ranges from 24 to 30 mμ (18), and an electron microscopic study of sectioned purified viral crystals has revealed dense ellipsoidal particles with a less dense outer zone, measuring 17 × 22 mμ (19). These observations compare well with the size and structure of ECHO type 9 virus as seen in thin sections of infected cells. It was not possible, however, to confirm the ellipsoidal shape of the virus. In favorable sections (Figs. 4, 11) the virus appears to consist of a dense central body surrounded by a delicate outer membrane. Such particles are approximately 22 mμ in diameter measured directly and 24 mμ determined as the center-to-center distance in close packed aggregates. The dense cores alone measure 13 to 15 mμ in diameter. Associated with these typical viral particles are numerous membrane-limited forms of considerably less density (Figs. 4, 5) which are also about 22 mμ in diameter.[1] Presumably such particles are incompletely invested with nucleic acid and are analogous to the non-infectious, nucleic acid–free fraction identified in the ultracentrifugal analysis of poliovirus (21). In this connection it is of interest that dense and incomplete forms have also been observed in electron microscopic studies of poliovirus infections (22)

[1] Viral particles of two distinct morphologic types have also been encountered in adenovirus-infected cells (20).

by means of the negative contrast technique (23). As seen in Fig. 5, incomplete viral particles often are very numerous in advanced stages of infection, suggesting that depletion of viral nucleic acid may occur as the cell approaches the phase of viral release and disintegration. Extracellular virus (Figs. 17 and 19) appears indistinguishable from the dense intracellular variety. Failure to find extracellular incomplete virus may reflect the inherent instability of this form, a possibility suggested by Horne and Nagington (22).

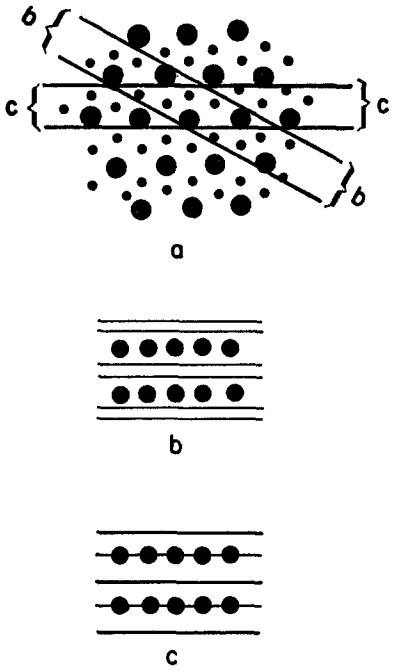

TEXT-FIG. 1. A drawing which shows the probable arrangement of viral particles and fibrils. 1 a A viral aggregate in cross-section. 1 b Longitudinal section, indicated *b-b* in 1 a. 1 c Longitudinal section *c-c* from 1 a.

II. Cytoplasmic Viral Aggregates.—

Intracytoplasmic crystalline arrays of enteroviral particles have been described for Coxsackie virus (6, 7), poliovirus (8, 9), an untyped ECHO (10), and ECHO 19 virus (11). In the case of ECHO 9 virus, there is an unusual, noncrystalline organization of intracytoplasmic viral particles upon a sheaf of fibrils. As indicated schematically in Text-fig. 1 a, fascicles of virus examined in cross-section display a regular hexagonal packing of the viral particles and fibrils (Figs. 7, 8). The relationship of fibril to virus as seen in longitudinal section (Figs. 3 to 5) is diagrammed in Text-figs. 1 b and 1 c. Generally two fibrils sep-

arate each row of virus but occasionally a single fibril lies between the rows while another is superimposed upon the virus. These contrasting images are readily reconciled by considering the relative section thickness (20 to 60 mμ), viral size (22 to 24 mμ) and the many possible planes of section. The two patterns displayed in Text-figs. 1 b and 1 c are derived from the hypothetical sections *b-b* and *c-c*, respectively, in Text Fig. 1 a.[2] It is notable that the fibrils appear to originate from the same granular template site as the virus itself (Fig. 10; see section V).

III. Stages of Infection.—

The sequence of consecutive stages during the cycle of infection was ascertained from detailed study by light microscopy of tissue cultures at specified intervals from the time of inoculation (1, 17). It was possible to order the electron micrographs in a comparable sequence without resorting to direct thick and thin section correlation (24) because the distinctive features in the development of the complete cellular lesion permitted recognition of each of the successive stages with equal facility in both light and electron micrographs.

IV. Cytopathic Effect.—

Several lines of evidence suggest that the nucleus is intimately involved in the development of many viruses (25), including some which differentiate within the cytoplasm (26–29). An early and brief increase in the rate of incorporation of P^{32} into nuclear RNA and DNA has been described during the growth of poliovirus in tissue culture (30). Furthermore, the earliest recognizable cytopathic effects of poliovirus (4, 5) and ECHO virus (1, 17), observed by light microscopy, are tinctorial and structural alterations in the nucleus. In this regard, electron microscopic study of ECHO 9 virus reveals progressive nuclear shrinkage, condensation of the chromatin, folding and accentuated fenestration of the nuclear membrane and dilatation of the perinuclear space (Figs. 1, 2, and 13). It should be emphasized, however, that on the basis of fluorescent antibody studies both of ECHO virus (17) and poliovirus (31), the nucleus does not appear to synthesize enteroviral protein.

The most striking early cytoplasmic alteration is the appearance of a mass of single and multiwalled vesicles in the juxtanuclear region. This mass eventually comes to displace both the altered nucleus and most of the normal cytoplasmic constituents (Fig. 1). A similar lesion has been clearly described for poliovirus infections (12) and undoubtedly represents the pale-staining eosinophilic body observed in light microscopic studies of ECHO virus-infected cells (1, 17) and previously described by Reissig (5) and others for poliovirus. Intracytoplasmic vacuolization has been reported to occur in the course of infection by a number of viruses. In the case of Western equine encephalomyelitis virus the vacuoles

[2] The assistance of Dr. Barbara Low in the interpretation of these patterns is gratefully acknowledged.

are clearly implicated in the process of viral morphogenesis (32), whereas in herpes simplex infections they appear to be involved in the transport and release of viral particles (33). The significance of the prominent vesicles and small vacuoles seen in ECHO virus infection is not known.

An increase in the number of free ribonucleoprotein granules is also characteristic of the infected cell (Fig. 1). During early stages, aggregates of ribonucleoprotein granules are often apposed to the nuclear membrane (Figs. 2, 13); later, large masses of such granules, which differ in structure from the virus (Fig. 12), are found throughout the cytoplasm, most commonly at the periphery (Figs. 12, 17, 18). These concentrations of ribonucleoprotein granules adequately account for the striking diffuse and granular cytoplasmic basophilia encountered in this (1) and other enteroviral infections (5, 34). No evidence was obtained in support of the suggestion that cytoplasmic particles originate from nucleolar substance (9).

An unusual finding is the frequent occurrence of numerous small dense granules, averaging 8 to 10 mμ in diameter, disposed upon the cristae of many otherwise unremarkable mitochondria (Fig. 16). As previously stated, the particles are considerably smaller than either the viral or nucleoprotein particles in the adjacent cytoplasm. No relationship between these granules and viral development has been ascertained.

V. Viral Differentiation and Release.—

An hypothesis regarding development and release of ECHO 9 virus appears justified on the basis of the morphologic data presented. Finely granular masses of electron-dense material, presumably a viral precursor, appear to serve as cytoplasmic template sites at which both fully mature and incomplete forms differentiate (Figs. 9 to 11). Fine filaments, of the same approximate diameter as the fibrils associated with fully formed viral aggregates, are occasionally seen within the template sites and the newly differentiated virus seems to be promptly oriented in typical linear arrays (Fig. 10). The differentiation of viral particles within cytoplasmic masses of precursor material has previously been described for several viruses of the pox group (35–38) and for reovirus (39). Whether the template sites are involved in the formation of viral precursors or represent focal deposits of previously synthesized viral material is unknown. The immunofluorescence studies of Buckley (31) suggest that enteroviral antigen is closely associated with areas of cytoplasmic basophilia which may, in turn, be equated with zones of increased ribonucleoprotein content. Viral particles have never been observed within the large masses of ribonucleoprotein granules and are only occasionally found in the vicinity of such nucleoprotein collections. Juxtaposition of virus and granule-bearing elements of the endoplasmic reticulum, observed by Stuart *et al.* (9) in studies of poliomyelitis and Coxsackie viruses, was rarely encountered. The relationship of ribonucleoprotein granule, endoplasmic reticulum and the virus remain obscure.

Prior to release, viral particles appear to free themselves of their accompanying fibrils and become dispersed, generally near the periphery of the cell (Figs. 15, 17). Most commonly, clusters of virus and fragments of cytoplasmic ground substance leave the cell through small rents in the plasma membrane, as seen in Fig. 17. Many such tears may occur in a single cell without evidence of severe disruption of its internal architecture (Fig. 18), accounting, perhaps, for the viability of enterovirus-infected cells during early phases of viral release (3). In addition, apparently viable cells shed cytoplasmic protrusions, containing virus, into the culture fluid (Figs. 18, 19). A similar mechanism has been observed in vital preparations of ECHO virus (17) and poliovirus-infected tissue cultures (3). The foregoing modes of release appear to be variants of a basic mechanism, namely, a weakening of the plasma membrane with resultant discrete or extensive rupture of the cell and extrusion of varying amounts of cytoplasmic material including virus. Finally, some cells (Fig. 20) undergo necrosis and disrupt with dispersion of virus.

SUMMARY

Sequential stages in the development and release of ECHO 9 virus have been illustrated and described. It is suggested that viral particles differentiate and become oriented in columns upon a fine filamentous lattice at cytoplasmic template sites which are distinct from the endoplasmic reticulum. Subsequently, virus is dispersed in the peripheral cytoplasm and gains egress from the cell through rents in the plasma membrane. Complete cellular disruption with viral release may supervene. The virus consists of a 13 to 15 mμ dense core and a poorly defined outer membrane, 22 to 24 mμ in diameter. Incomplete forms, lacking the core, are observed in the cytoplasm but have not been seen in the extracellular space.

BIBLIOGRAPHY

1. Rifkind, R. A., Godman, G. C., Howe, C., Morgan, C., and Rose, H. M., ECHO 9 virus in tissue culture observed by light and electron microscopy, *Virology*, 1960, **12**, 331.
2. Love, R., Cytopathology of virus-infected tumor cells, *Ann. New York Acad. Sc.*, 1959, **81**, 101.
3. Barski, G., Robineaux, R., and Endo, M., Phase contrast cinematography of cellular lesion produced by poliomyelitis virus *in vitro*, *Proc. Soc. Exp. Biol. and Med.*, 1955, **88**, 57.
4. Dunnebacke, T. H., Correlation of the stage of cytopathic change with the release of poliomyelitis virus, *Virology*, 1956, **2**, 399.
5. Reissig, M., Howes, D. W., and Melnick, J. L., Sequence of morphological changes in epithelial cell cultures infected with poliovirus, *J. Exp. Med.*, 1956, **104**, 289.
6. Morgan, C., Howe, C., and Rose, H. M., Intracellular crystals of Coxsackie virus viewed in the electron microscope, *Virology*, 1959, **9**, 145.

7. Fogh, J., and Stuart, D. C., Jr., Intracytoplasmic crystalline and noncrystalline patterns of Coxsackie virus in FL cells, *Virology*, 1959, **9,** 705.
8. Stuart, D. C., Jr., and Fogh, J., Intracellular crystals of poliovirus in HeLa cells, *Virology*, 1960, **11,** 308.
9. Stuart, D. C., Jr., and Fogh, J., Micromorphology of FL cells infected with polio- and Coxsackie viruses, *Virology*, 1961, **13,** 177.
10. Stuart, D. C., Jr., Fogh, J., and Plager, H., Cytoplasmic crystals in FL cells infected with an unclassified enteric virus (presumbably a new type of ECHO virus), *Virology*, 1960, **12,** 321.
11. Nunez-Montiel, O., and Weibel, J., Electron microscope study of ECHO 19 virus infection in monkey kidney cells, *J. Biophysic. and Biochem. Cytol.*, 1960, **8,** 291.
12. Kallman, F., Williams, R. C., Dulbecco, R., and Vogt, M., Fine structure of changes produced in cultured cells sampled at specified intervals during a single growth cycle of polio virus, *J. Biophysic. and Biochem. Cytol.*, 1958, **4,** 301.
13. Melnick, J. L., Tissue culture techniques and their application to original isolation, growth and assay of poliomyelitis and orphan viruses, *Ann. New York Acad. Med.*, 1955, **61,** 754.
14. Morgan, C., Howe, C., Rose, H. M., and Moore, D. H., Structure and development of viruses observed in the electron microscope. IV. Viruses of the RI-APC group, *J. Biophysic. and Biochem. Cytol.*, 1956, **2,** 351.
15. Dalton, A. J., and Zeigel, R. F., A simplified method of staining thin sections of biological material with lead hydroxide for electron microscopy, *J. Biophysic. and Biochem. Cytol.*, 1960, **7,** 409.
16. Vogel, J., and Shelokov, A., Adsorption-hemagglutination test for influenza virus in monkey kidney tissue culture, *Science*, 1957, **126,** 358.
17. Godman, G. C., data in preparation.
18. Benyesh, M., Pollard, E. C., Opton, E. M., Black, F. L., Bellamy, W. D., and Melnick, J. L., Size and structure of ECHO, poliomyelitis, and measles virus determined by ionizing radiation and ultrafiltration, *Virology*, 1958, **5,** 256.
19. Hanzon, V., and Philipson, L., Ultrastructure and spatial arrangement of ECHO virus particles in purified preparations, *J. Ultrastructure Research*, 1960, **3,** 420.
20. Morgan, C., and Rose, H. M., Electron microscopic observations on adenoviruses and viruses of the influenza group, Virus Growth and Variation, *9th Symp. Soc. Gen. Microbiol.*, 1959, 256.
21. Le Bouvier, G. L., Schwerdt, D. E., and Schaffer, F. L., Specific precipitates in agar with purified poliovirus, *Virology*, 1957, **4,** 590.
22. Horne, R. W., and Nagington, J., Electron microscope studies of the development and structure of poliomyelitis virus, *J. Molecular Biol.*, 1959, **1,** 333.
23. Brenner, S., and Horne, R. W., A negative staining method for high resolution electron microscopy of viruses, *Biochim. et Biophysica Acta*, 1959, **34,** 103.
24. Bloch, D. P., Morgan, C., Godman, G. C., Howe, C., and Rose, H. M., A correlated histochemical and electron microscopic study of the intranuclear crystalline aggregates of adenovirus (RI-APC virus) in HeLa cells, *J. Biophysic. and Biochem. Cytol.*, 1957, **3,** 1.

25. Rose, H. M., and Morgan, C., Fine structure of virus-infected cells, *Ann. Rev. Microbiol.*, 1960, **14,** 217.
26. Watson, B. D., and Coons, A. H., Studies of influenza virus infection in the chick embryo using fluorescent antibody, *J. Exp. Med.*, 1954, **99,** 419.
27. Liu, C., Studies on influenza infection in ferrets by means of fluorescein-labelled antibody. II. The role of "soluble antigen" in nuclear fluorescence and cross-reactions, *J. Exp. Med.*, 1955, **101,** 677.
28. Breitenfeld, P. M., and Schafer, W., The formation of fowl plague virus antigens in infected cells, as studied with fluorescent antibodies, *Virology*, 1957, **4,** 328.
29. Morgan, C., and Rose, H. M., Electron-microscopic observations on adeno-viruses and viruses of the influenza group, *in* Virus Growth and Variation, *9th Symp. Soc. Gen. Microbiol.*, 1959, 256.
30. Maassab, H. F., and Ackermann, W. W., Nucleic acid metabolism of virus-infected HeLa cells, *Ann. New York Acad. Sc.*, 1959, **81,** 29.
31. Buckley, S. M., Cytopathology of poliomyelitis virus in tissue culture. Fluorescent antibody and tinctorial studies, *Am. J. Path.*, 1957, **33,** 691.
32. Morgan, C., Howe, C., and Rose, H. M., Structure and development of viruses as observed in the electron microscope. V. Western equine encephalomyelitis virus, *J. Exp. Med.*, 1961, **113,** 219.
33. Morgan, C., Rose, H. M., Holden, M., and Jones, E. P., Electron microscopic observations on the development of herpes simplex virus, *J. Exp. Med.*, 1959, **110,** 643.
34. Ackermann, W. W., Rabson, A., and Kurtz, H., Growth characteristics of poliomyelitis virus in HeLa cell cultures: Lack of parallelism in cellular injury and virus increase, *J. Exp. Med.*, 1954, **100,** 437.
35. Morgan, C., Ellison, S. A., Rose, H. M., and Moore, D. H., Structure and development of viruses observed in the electron microscope. II. Vaccinia and fowl pox viruses, *J. Exp. Med.*, 1954, **100,** 301.
36. Bernhard, W., Bauer, A., Harel, J., and Oberling, C., Les formes intracytoplasmiques du virus fibromateux de Shope, *Bull. Cancer*, 1954, **41,** 423.
37. Ozaki, Y., and Hagashi, N., Studies on the growth of viruses ectromelia and vaccinia in strain L cells and HeLa cells, *Ann. Rep. Inst. Virus Research*, Kyoto Univ., 1959, Ser. B, **2,** 65.
38. Dourmashkin, R., and Bernhard, W., A study with the electron microscope of the skin tumour of molluscum contagiosum, *J. Ultrastructure Research*, 1959, **3,** 11.
39. Tournier, P., and Plissier, M., Le developpement intracellulaire du reovirus observe au microscope electronique, *Presse méd.*, 1960, **68,** 683.

EXPLANATION OF PLATES

PLATE 1

FIG. 1. A relatively early stage of infection. The contorted nucleus contains marginated chromatin and a single nucleolus (*Nu*). There is a mass of small vesicles below the nucleus displacing mitochondria (*m*) and endoplasmic reticulum (*er*) to the periphery of the cell. No virus is seen. × 14,000.

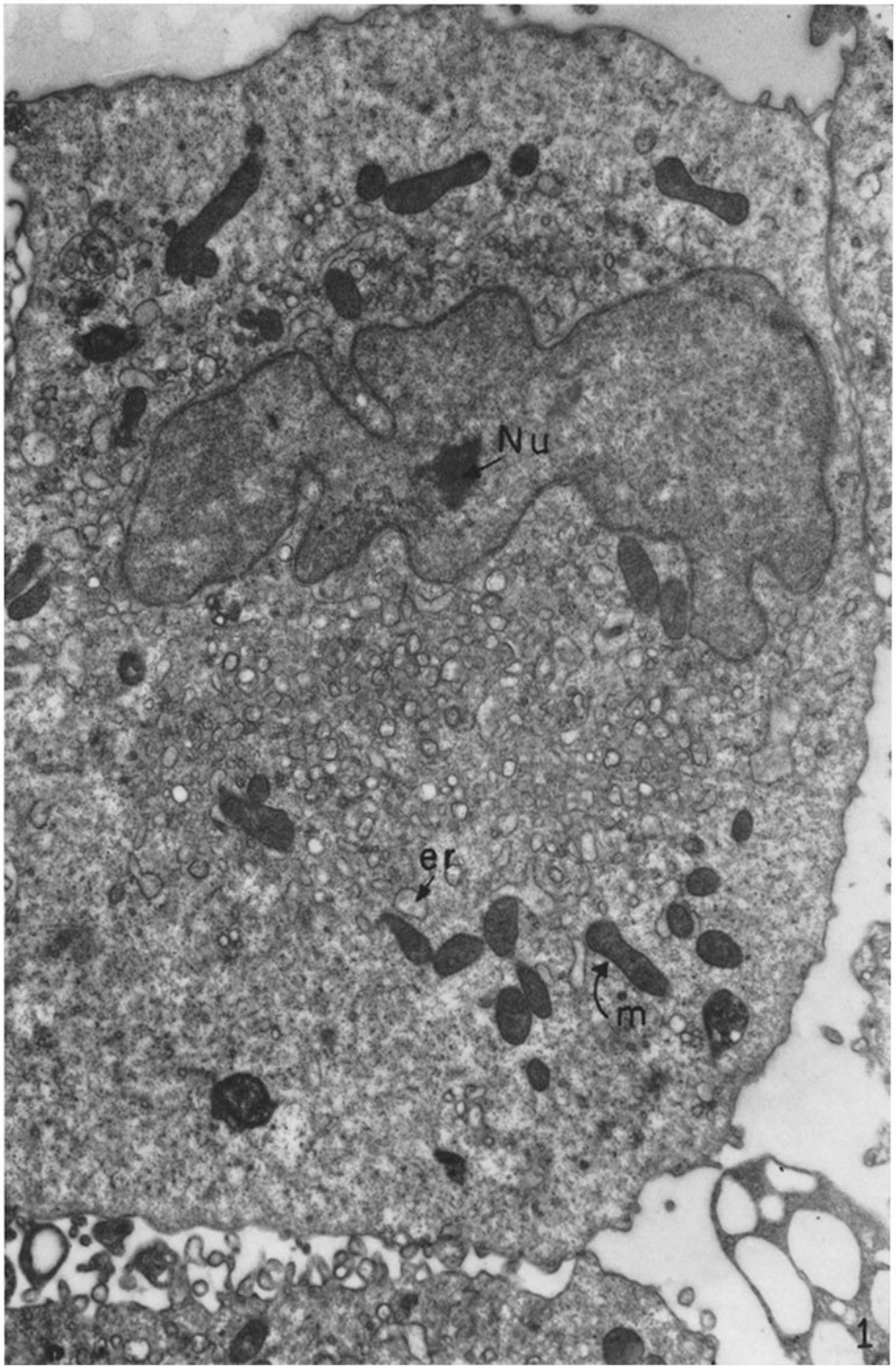

(Rifkind *et al.*: ECHO virus type 9 observed in electron microscope)

PLATE 2

FIG. 2. A more advanced stage of infection. The cell contains a markedly condensed and collapsed nucleus (*N*), large clusters of dense granules (*g*) and a central mass of vesicles and vacuoles. Four linear aggregates of viral particles are indicated by arrows. × 16,000.

PLATE 3

FIG. 3. Four viral arrays near a large cytoplasmic vacuole. Fine filaments course between the rows of virus and mingle with similar fibrils in the adjacent cytoplasm. × 58,000.

PLATE 4

FIG. 4. The upper viral aggregate from the preceding micrograph at higher magnification. Dense particles with delicate outer coats (arrows) as well as membrane-limited but less dense forms are aligned between parallel filaments. One or two filaments separate each viral row. × 230,000.

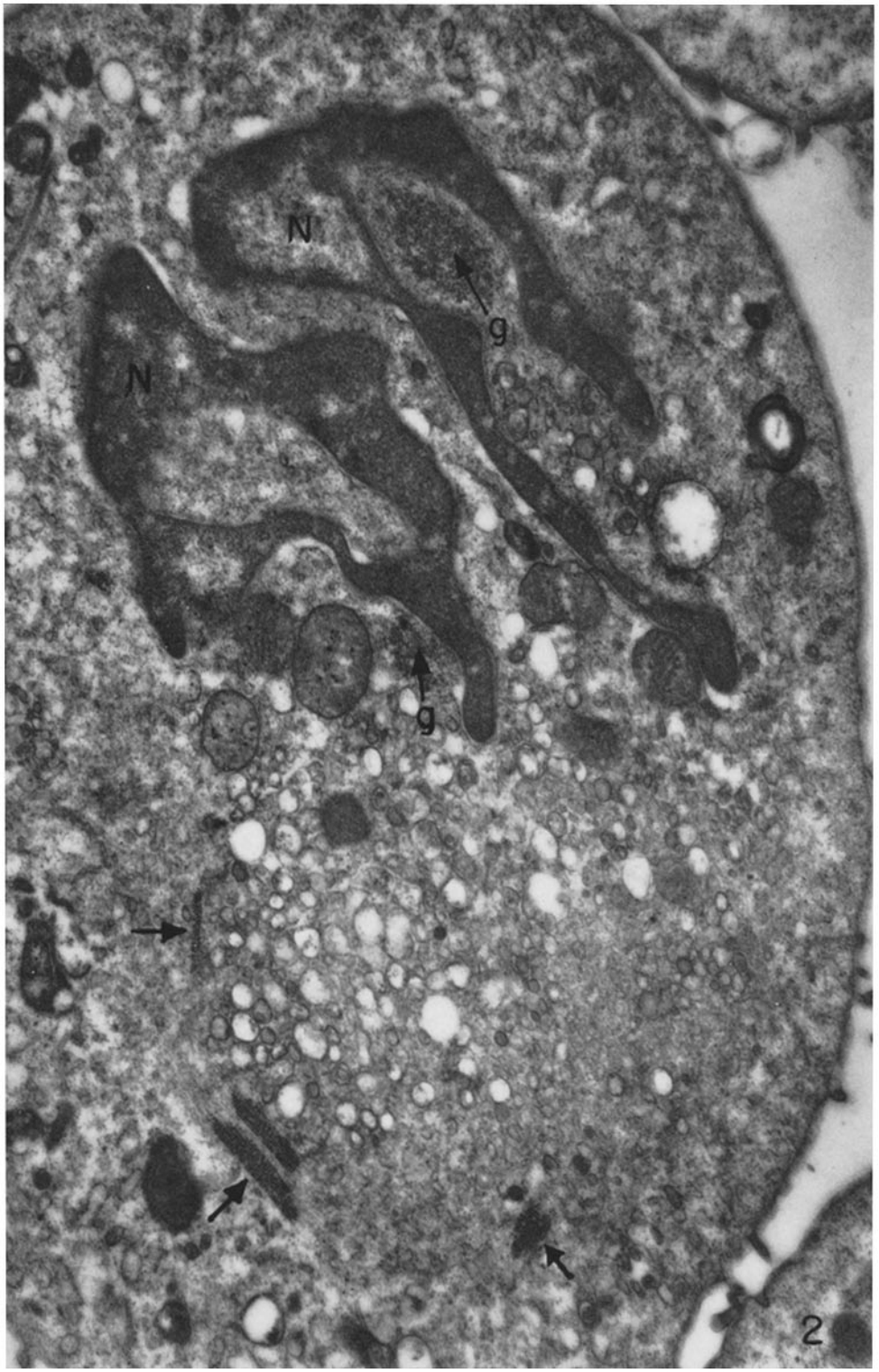

(Rifkind *et al.*: ECHO virus type 9 observed in electron microscope)

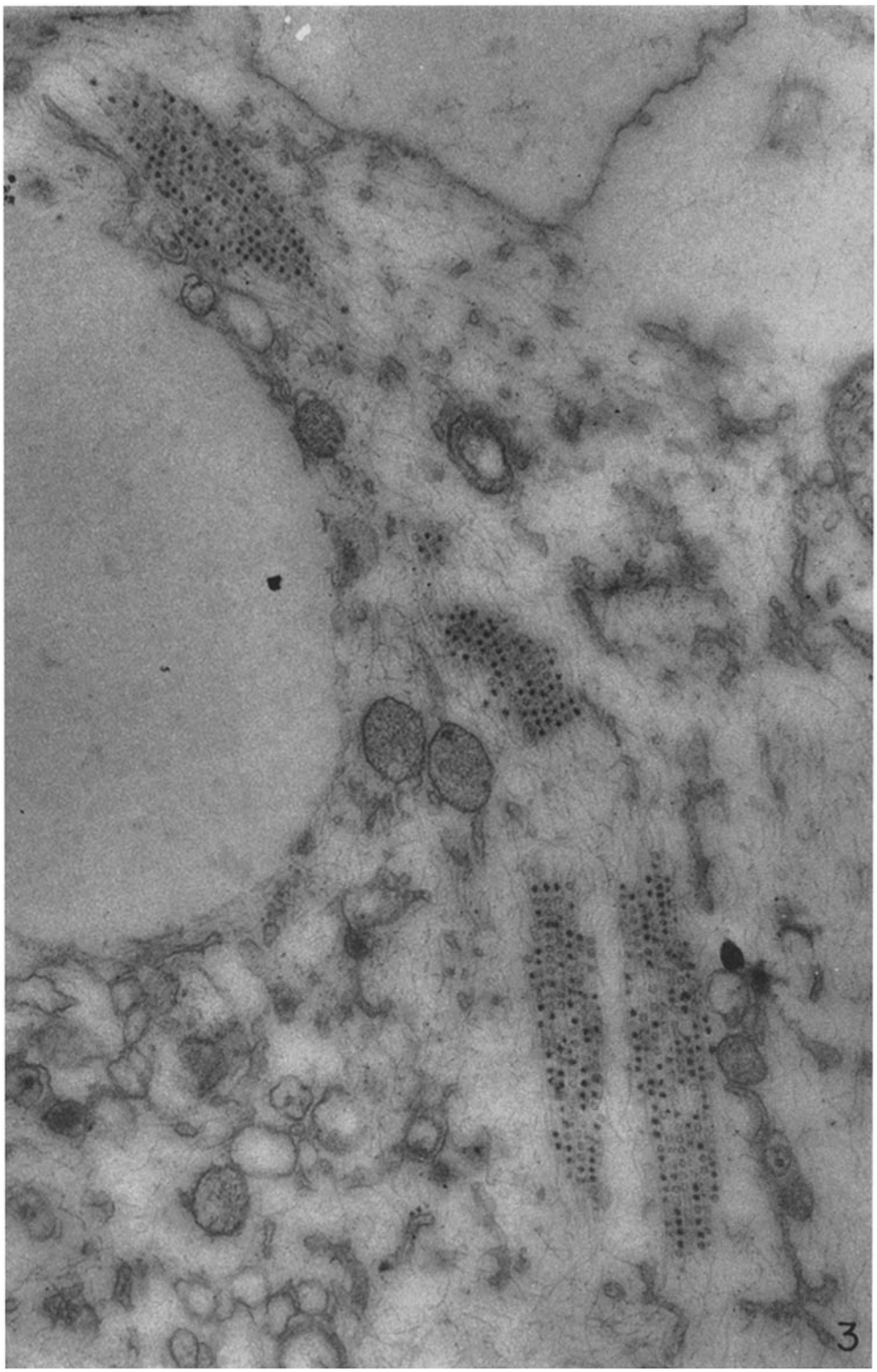

(Rifkind *et al.*: ECHO virus type 9 observed in electron microscope)

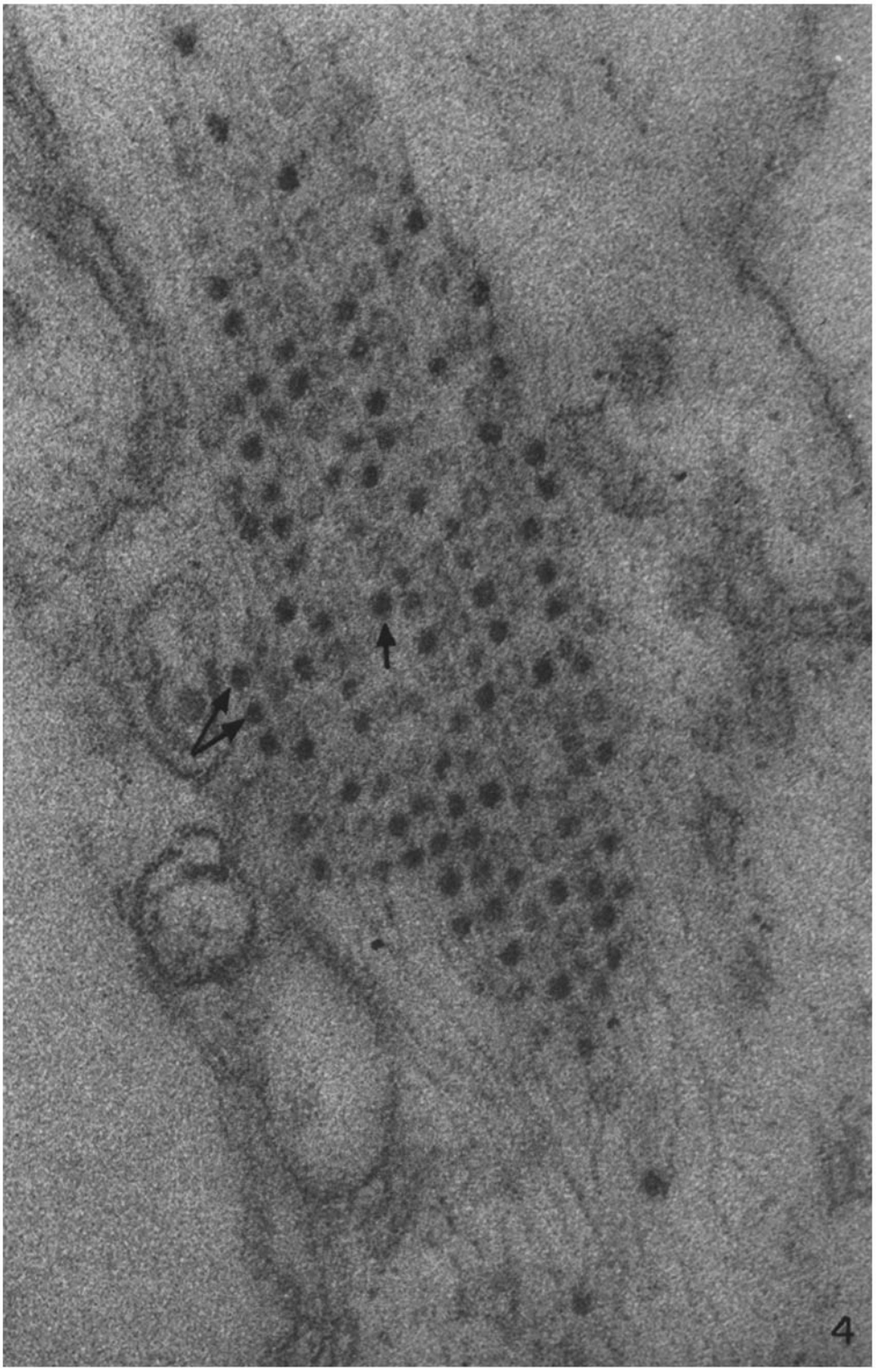

(Rifkind *et al.*: ECHO virus type 9 observed in electron microscope)

PLATE 5

FIG. 5. An advanced stage of infection with fragmented and distorted mitochondria (*m*) and endoplasmic reticulum (*er*). Most cytoplasmic ground substance has been lost. Two viral arrays, composed predominantly of the less dense (incomplete) particles, are oriented upon fibrils which are coextensive with a network of identical fibrils free in the cytoplasm. × 43,000.

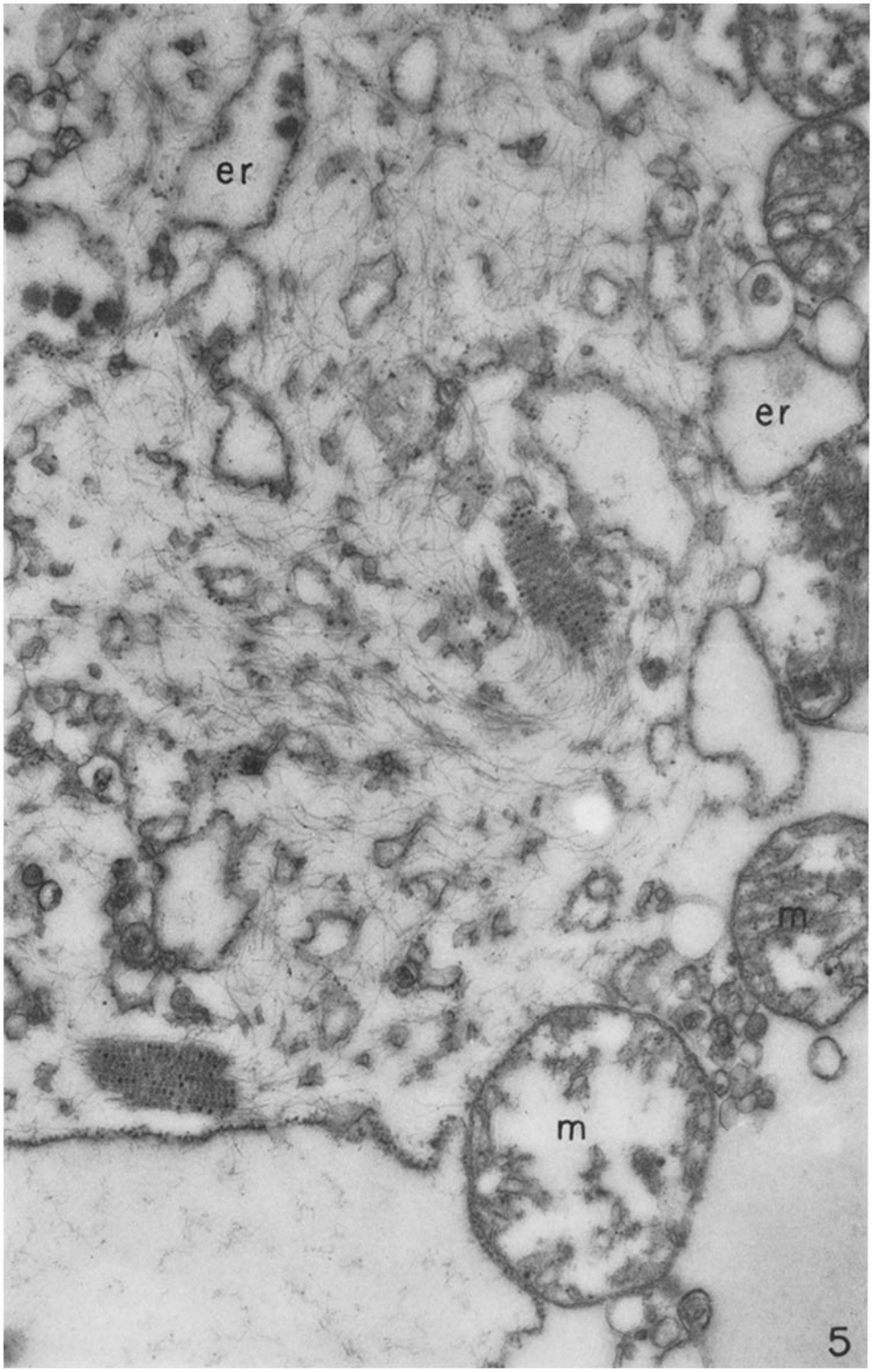

(Rifkind *et al.*: ECHO virus type 9 observed in electron microscope)

PLATE 6

FIG. 6. A moderately advanced stage of infection which displays a condensed and convoluted nucleus (*N*), cytoplasmic vacuolization and three viral arrays (labelled *A*, *B*, and *C*). Aggregate *A* is cut in longitudinal section, parallel to its fibrils, whereas *B* and *C* are in cross end oblique section, respectively. × 38,000.

FIG. 7. The cross-sectioned viral aggregate, labelled *B* in Fig. 6, which displays a roughly hexagonal outline. The viral particles are generally surrounded by 6 other viral particles and by 6 transected fibrils represented by small, punctuate densities. × 140,000.

FIG. 8. Another cross-sectioned viral array. The characteristic relationship of 6 fibrils to each viral particle is indicated by arrows. × 186,000. INSET: A viral particle and 6 surrounding fibrils (arrows). × 258,000.

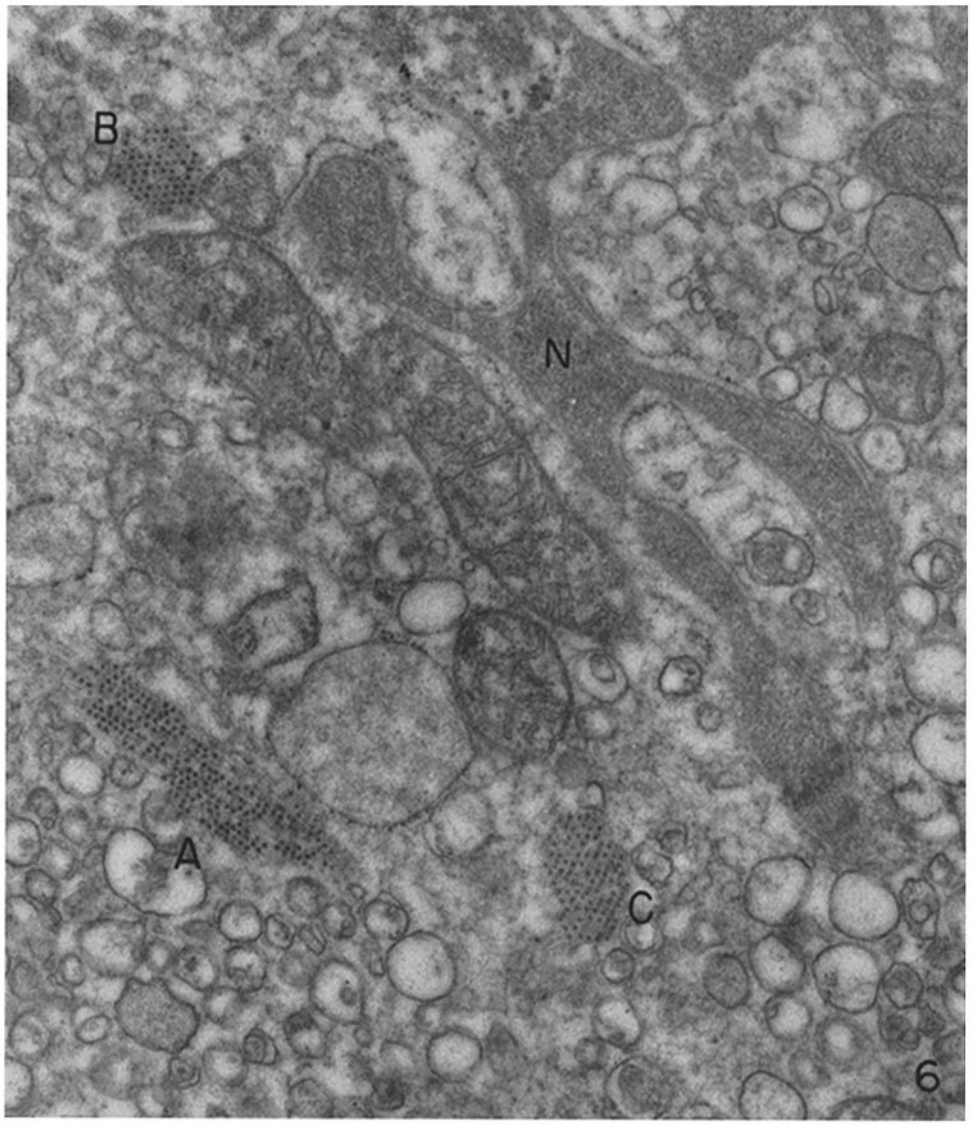

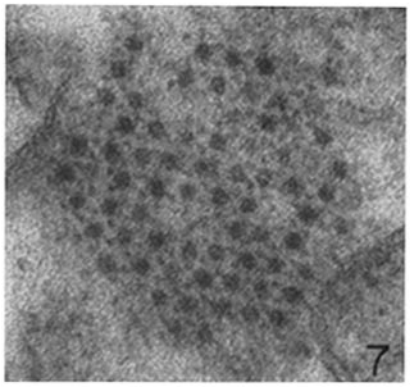

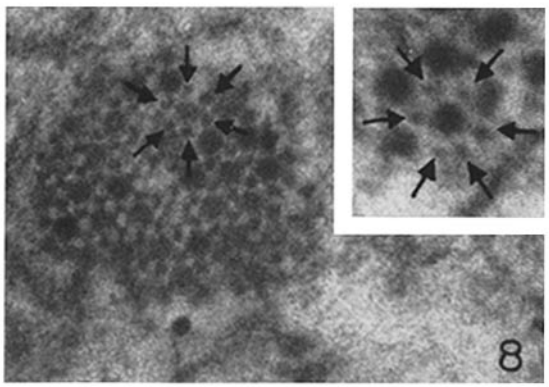

(Rifkind *et al.*: ECHO virus type 9 observed in electron microscope)

PLATE 7

FIG. 9. Six finely granular cytoplasmic masses, 4 of which (*A* to *D*) are intimately associated with typical viral arrays. × 51,000.

FIG. 10. Granular masses *C* and *D* from the preceding micrograph at higher magnification. A large, wedge-shaped viral array at the left is embedded within the finely granular and filamentous material of the mass. Several particles (arrows) display an outer membrane. Transected fibrils lie between the viral particles. × 113,000.

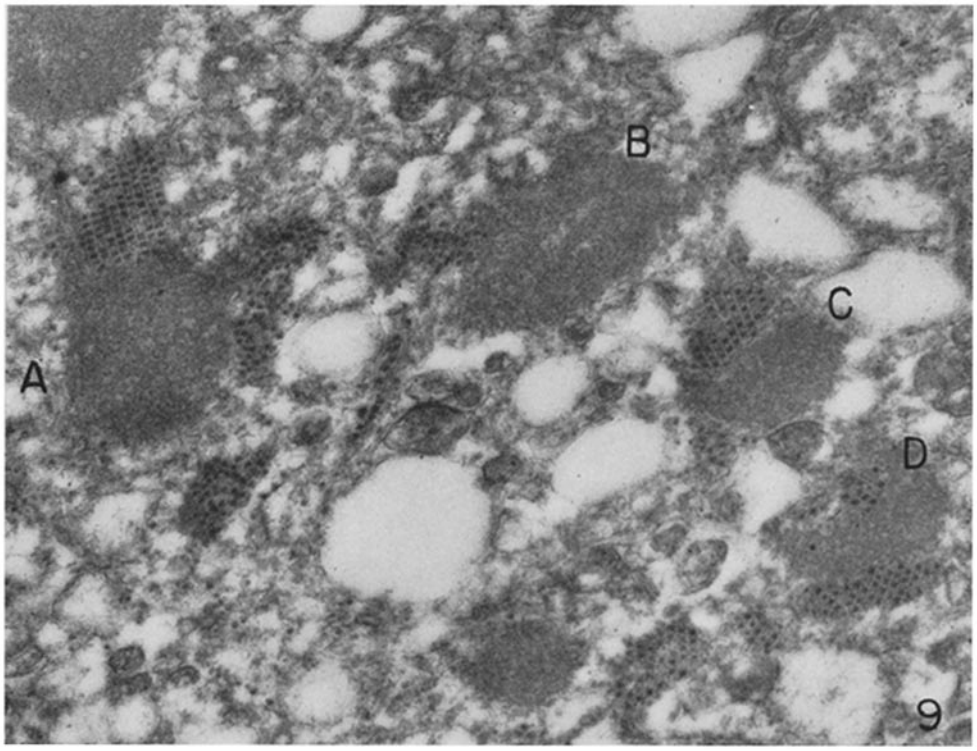

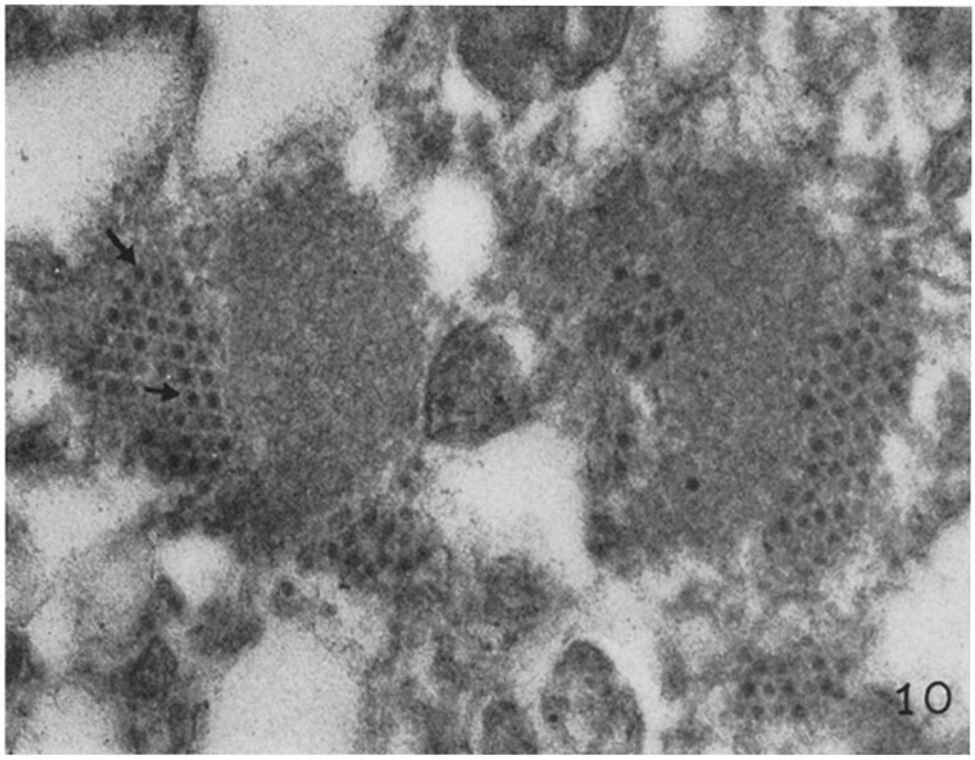

(Rifkind *et al.*: ECHO virus type 9 observed in electron microscope)

PLATE 8

FIG. 11. Two granular and filamentous masses and associated viral arrays from another cell. Both dense and incomplete viral particles are apparent. × 93,000. INSET: A membrane-coated, dense viral particle lying within the granular matrix. × 213,000.

(Rifkind *et al.*: ECHO virus type 9 observed in electron microscope)

PLATE 9

FIG. 12. An area of cytoplasm with a flat cisternal element of the endoplasmic reticulum and a large aggregate of irregular, variably dense, ribonucleoprotein particles. In the lower third, 3 cross-sectioned arrays of uniformly round, dense viral particles and fibrillar profiles. × 135,000.

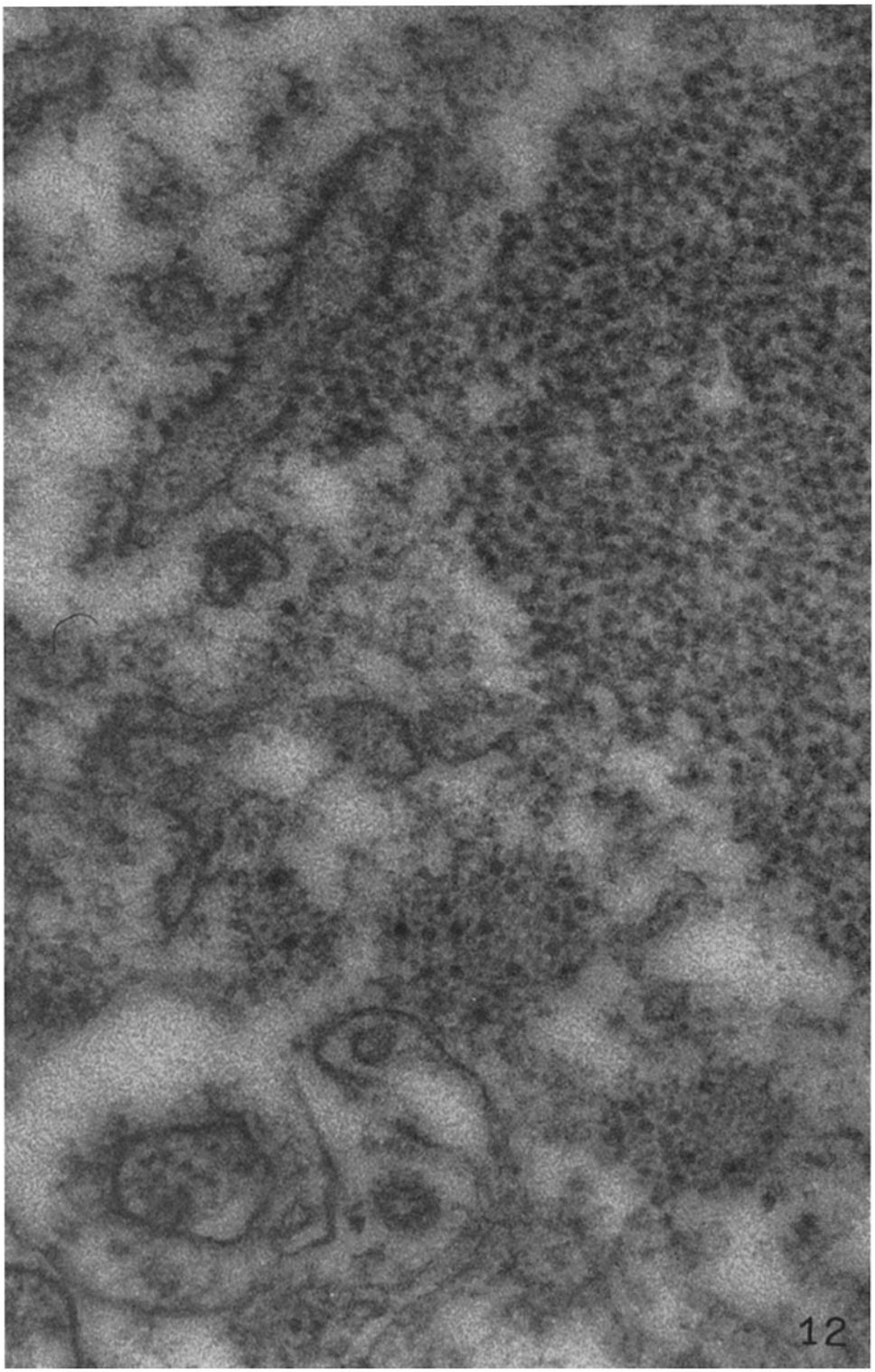

(Rifkind *et al.*: ECHO virus type 9 observed in electron microscope)

PLATE 10

FIG. 13. A collection of dense granules in the cytoplasm adjacent to a characteristically distorted nucleus (*N*). Nuclear fenestrations adjacent to rarefactions in the chromatin are evident. Several mitochondria containing small granules are seen at the left. Two small viral arrays are indicated by *v*. × 38,000.

FIG. 14. Part of the nucleus of Fig. 13 at higher magnification. The widened perinuclear space is bordered by a granule-encrusted outer nuclear membrane. × 77,000.

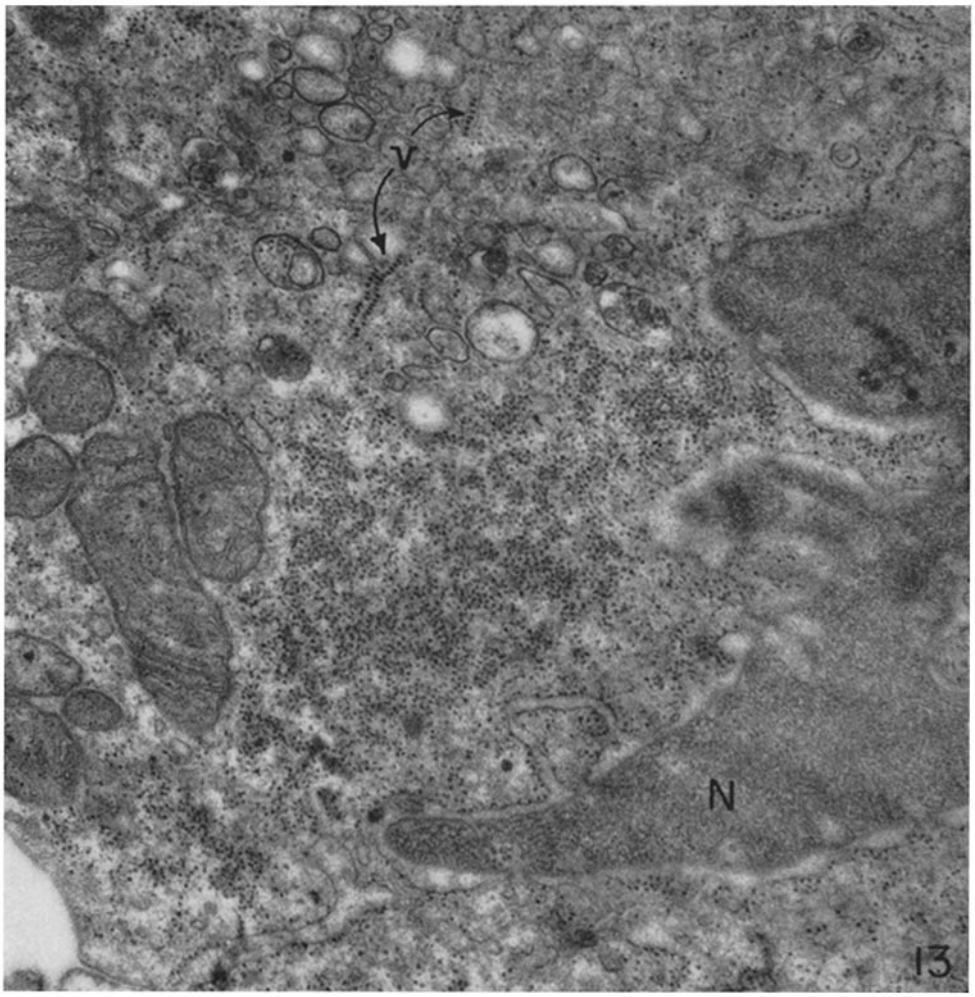

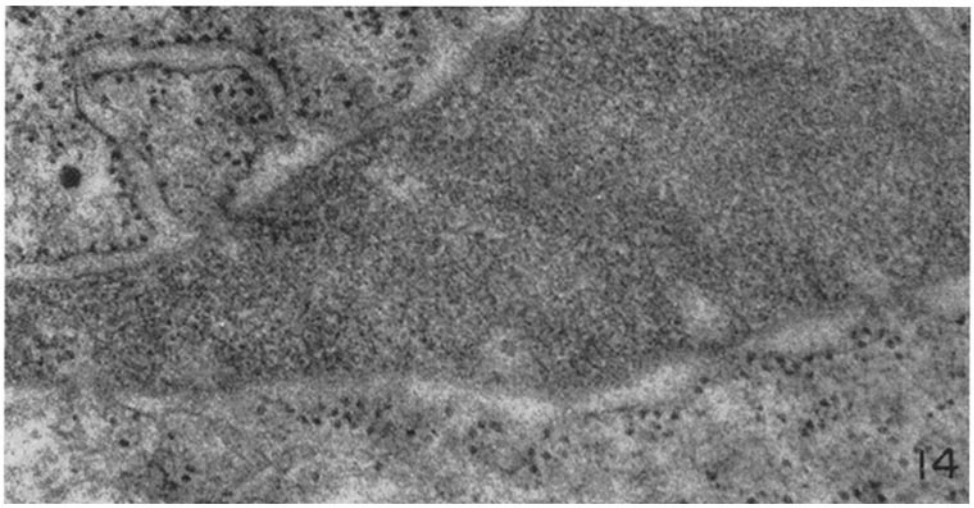

(Rifkind *et al.*: ECHO virus type 9 observed in electron microscope)

PLATE 11

FIG. 15. Cytoplasm of the infected cell with a long linear viral array in the center. Small clusters of virus displaying only remnants of a fibrillar lattice are indicated by arrows. × 24,000.

FIG. 16. Two mitochondria at the top of Fig. 15, seen at higher magnification. Numerous small dense granules are aligned upon the cristae mitochondriales. × 93,000.

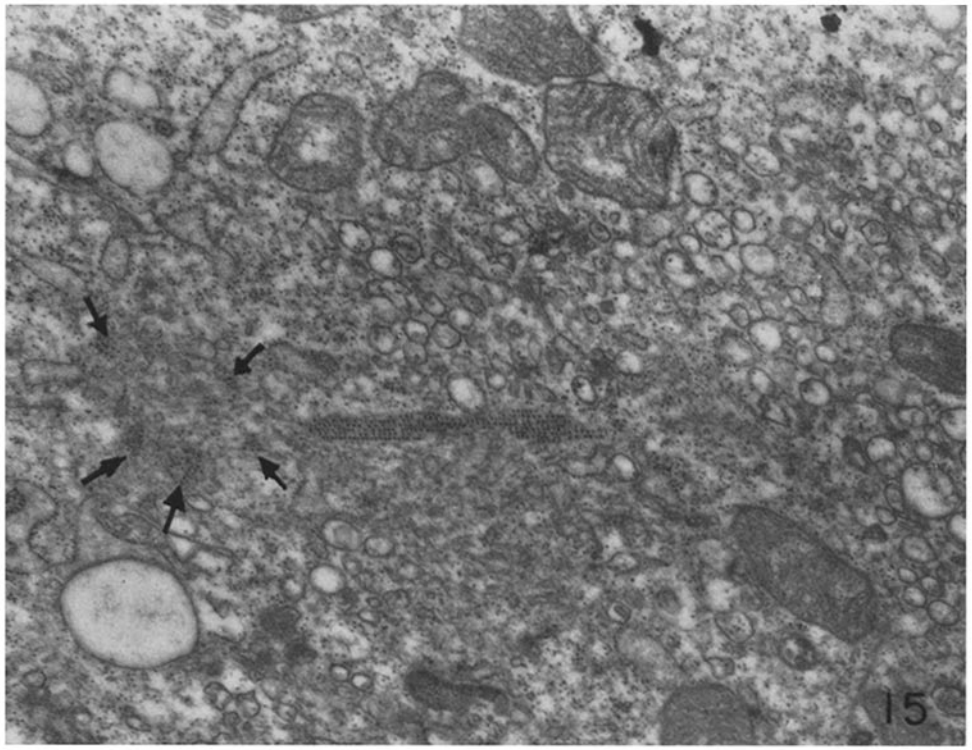

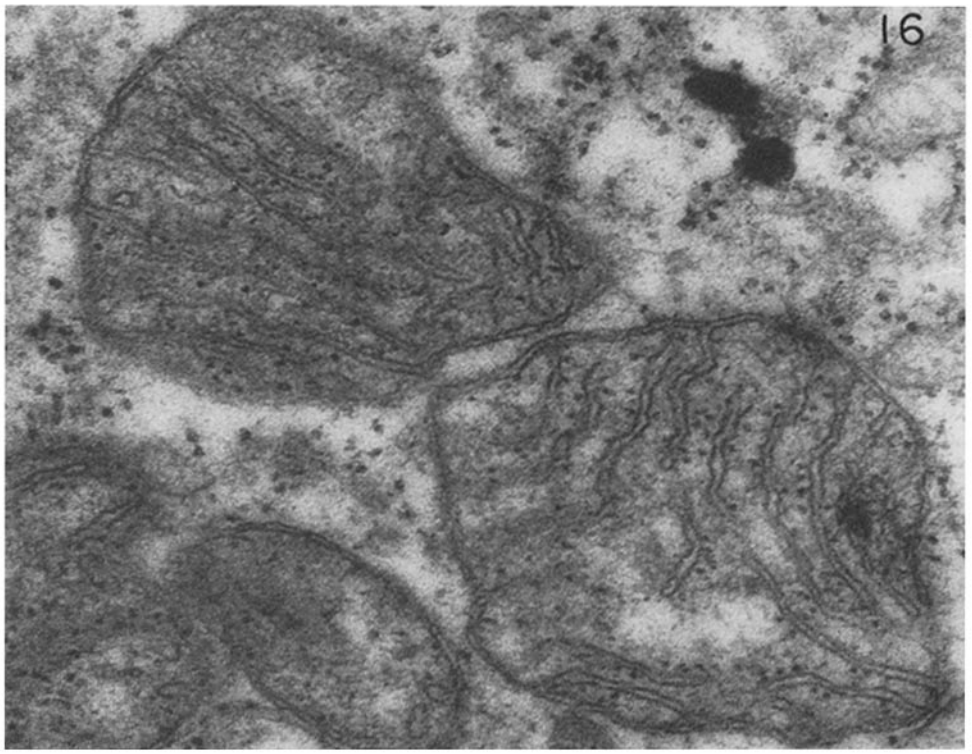

(Rifkind *et al.*: ECHO virus type 9 observed in electron microscope)

PLATE 12

FIG. 17. The plasma membranes of two adjacent cells traverse the plate diagonally. Small clusters of virus lying just beneath the plasma membrane on the right are marked by arrows. Groups of extracellular viral particles lie adjacent to discrete rents in the plasma membranes. × 92,000.

PLATE 13

FIG. 18. A large cytoplasmic process (*P*) appears to have been torn from the surface of a cell with release of numerous viral particles. Other aggregates of extracellular virus are indicated by arrows. × 29,000.

PLATE 14

FIG. 19. The avulsed cytoplasmic process and extracellular virus, shown in Fig. 18, at higher magnification. Above and toward the right several viral particles remain in the cytoplasmic substance. × 81,000.

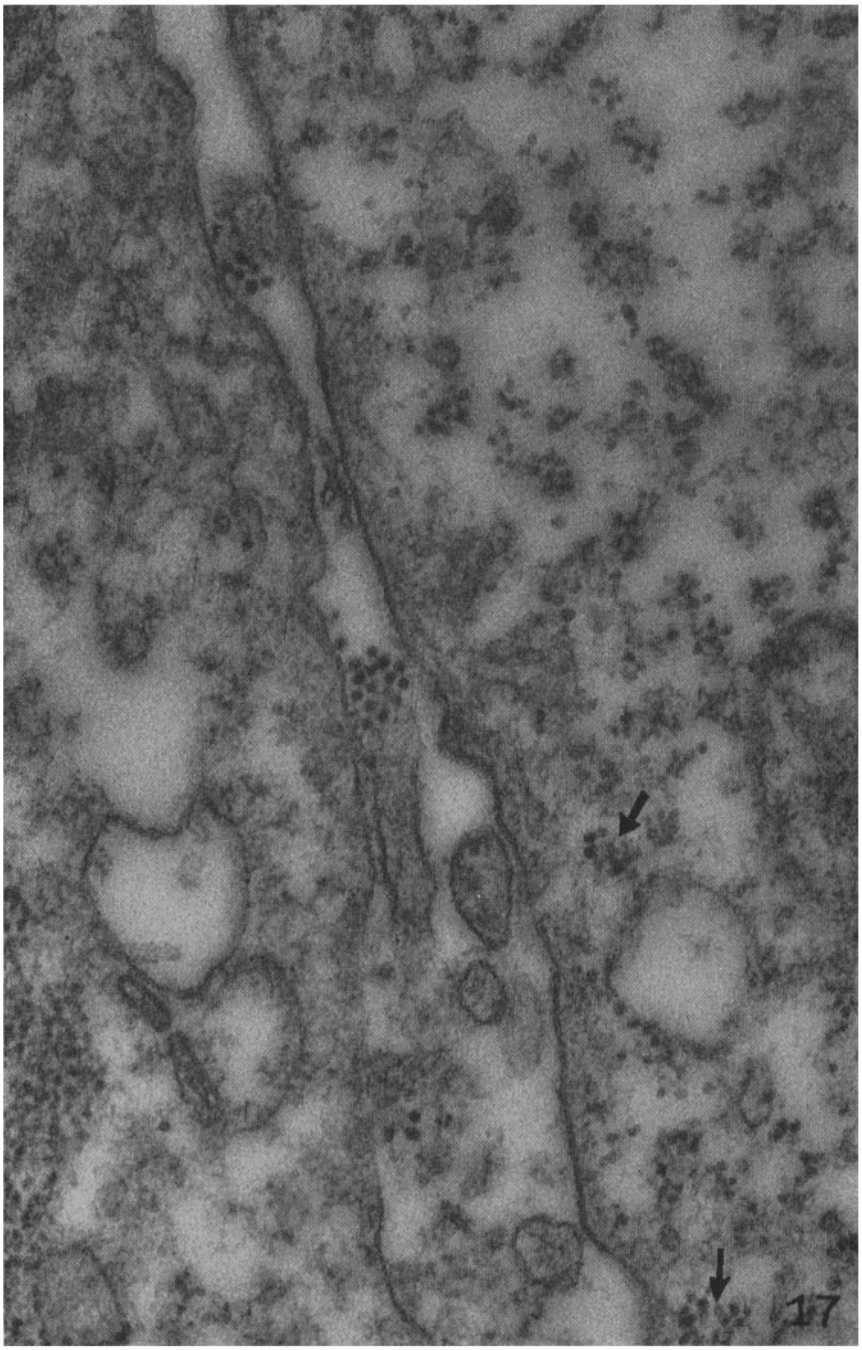

(Rifkind *et al.*: ECHO virus type 9 observed in electron microscope)

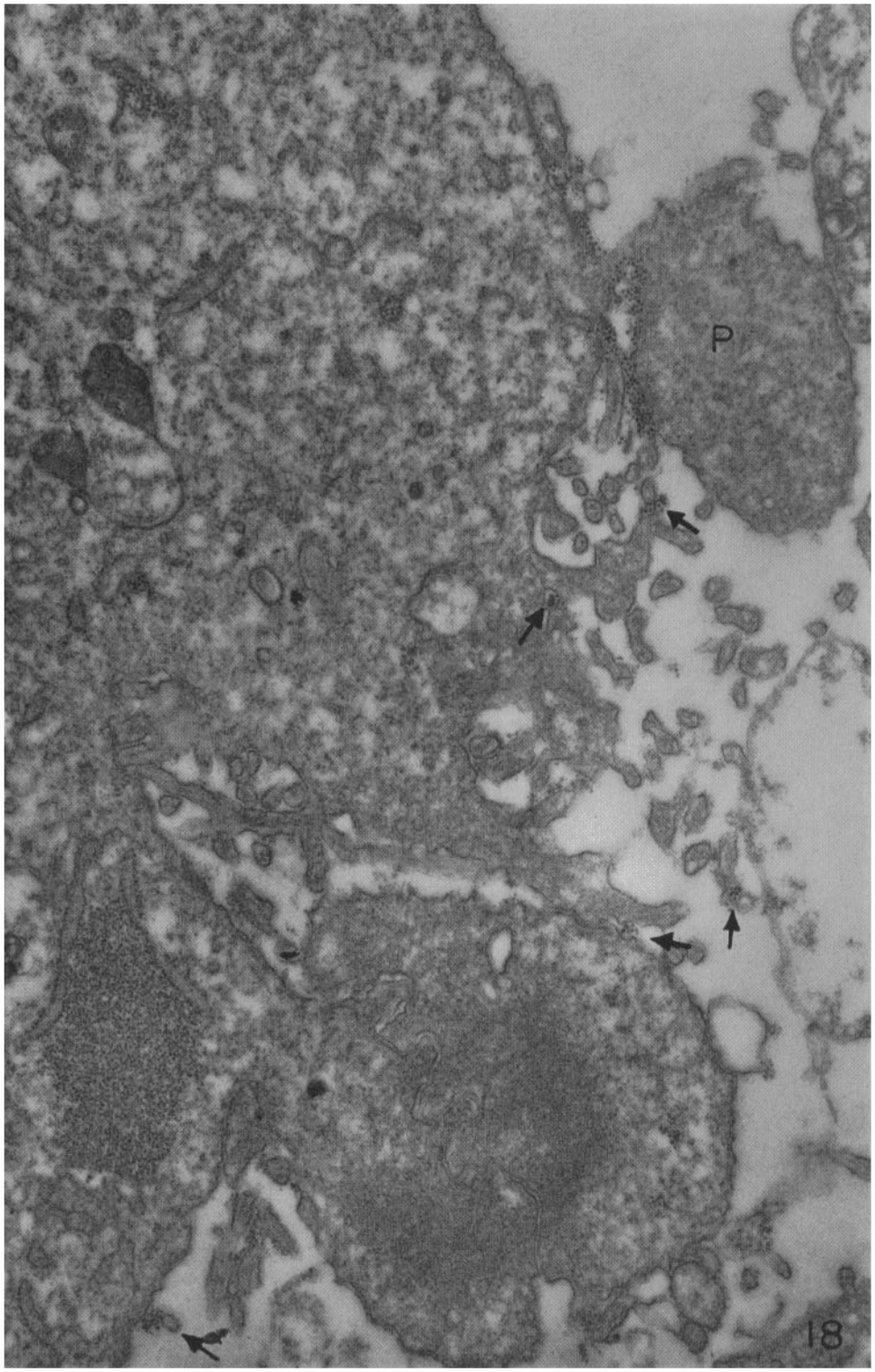

(Rifkind *et al.*: ECHO virus type 9 observed in electron microscope)

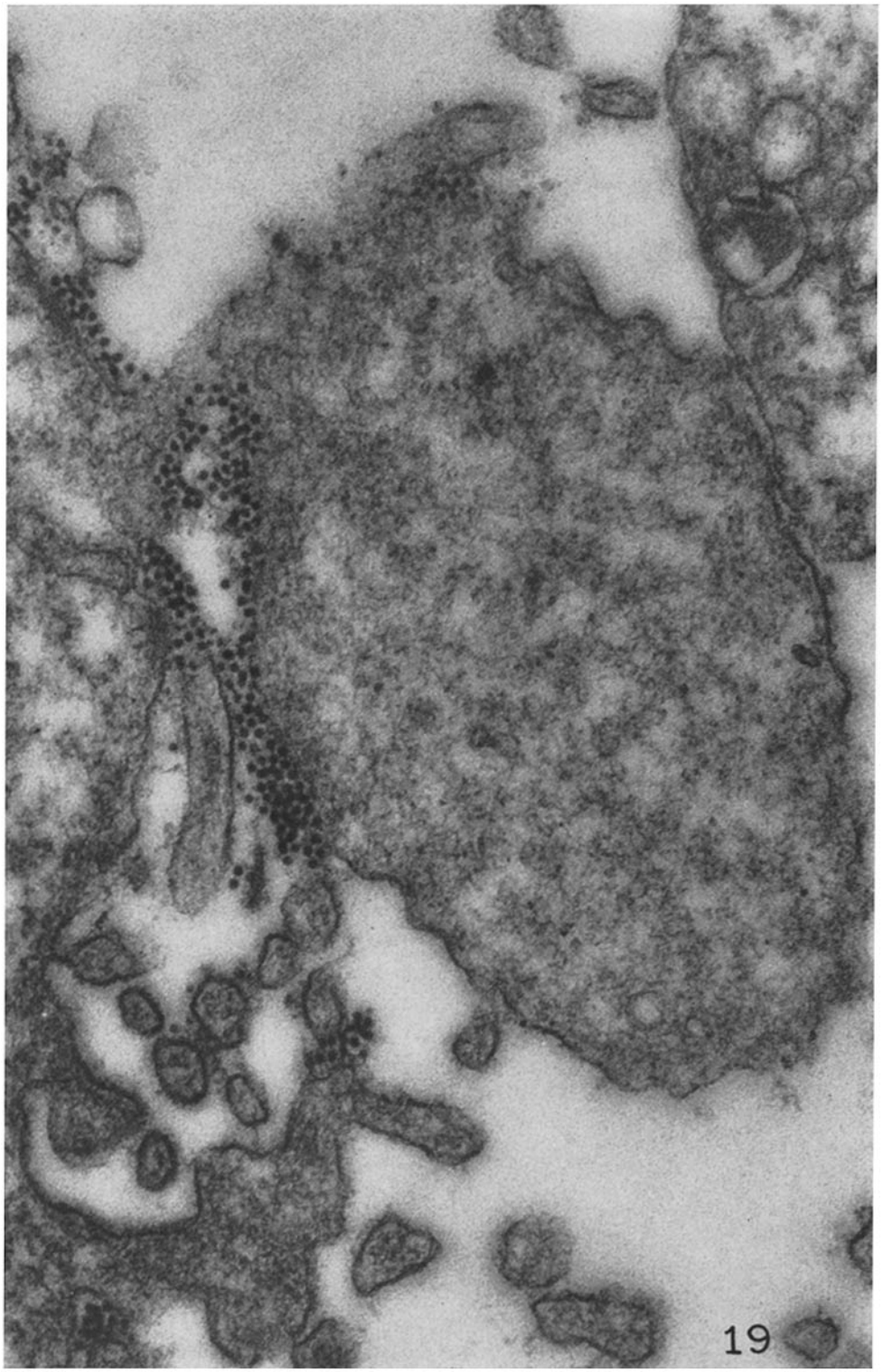

(Rifkind *et al.*: ECHO virus type 9 observed in electron microscope)

PLATE 15

FIG. 20. A disrupted cell. Many clusters of virus and cytoplasmic debris appear to be in process of dispersion into the extracellular space. × 39,000.

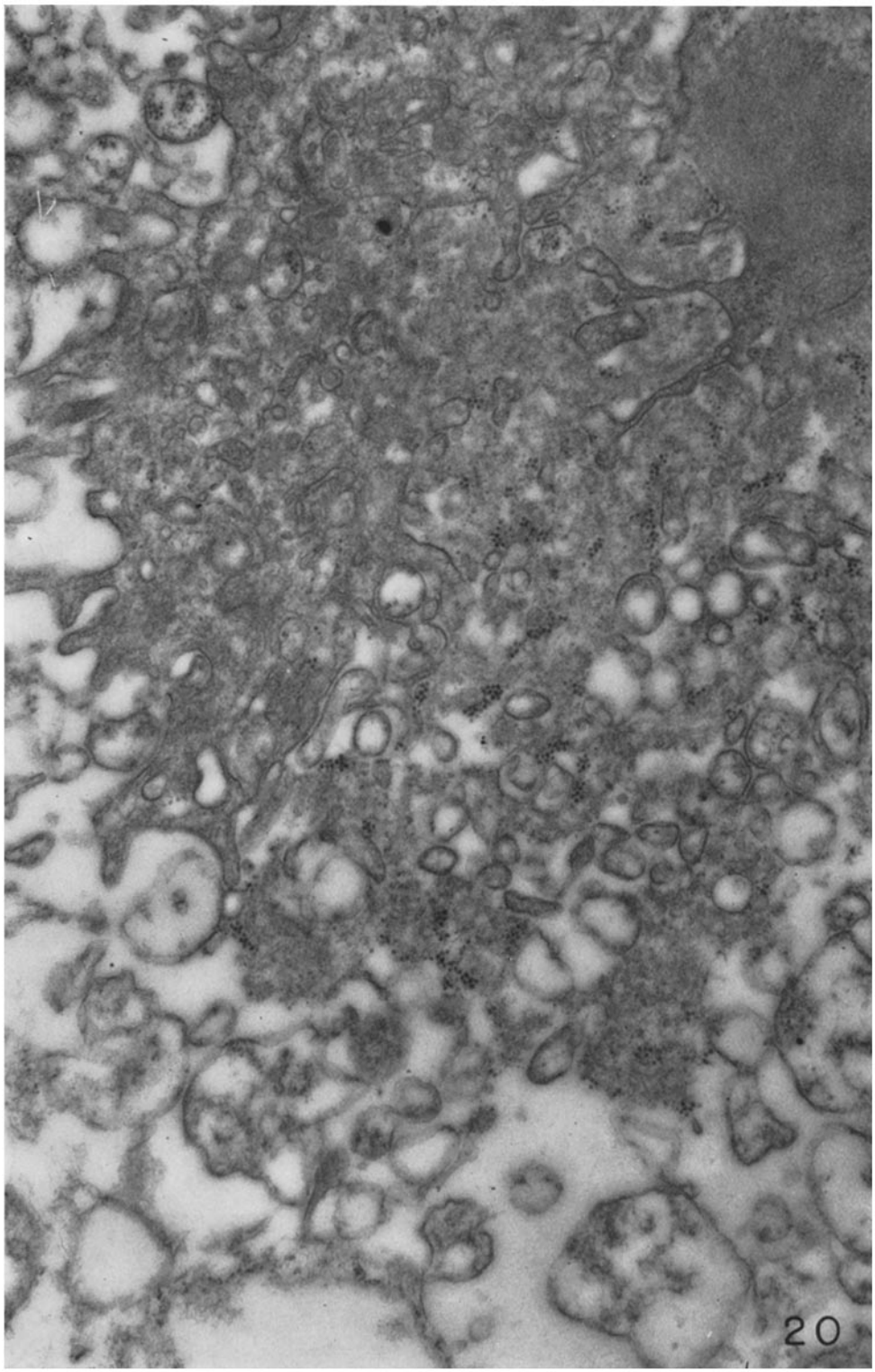

(Rifkind *et al.*: ECHO virus type 9 observed in electron microscope)